

Diffractive structure functions from HERA

Vincenzo Monaco

Università di Torino and INFN, Via Giuria 1, 10125 Torino, Italy

Recent results on diffraction at HERA are presented on behalf of the H1 and ZEUS Collaborations, focusing on the measurement of the inclusive diffractive cross section and on the study of two and three jets produced in diffractive ep scattering.

1 Inclusive diffraction

At HERA, a significant fraction of neutral-current deep inelastic scattering (DIS) events is characterized by a large rapidity gap between the hadronic state measured in the detector and the proton direction. These events result predominantly from diffractive dissociation of the virtual photon; the lack of QCD radiation in the proton direction is interpreted in terms of the exchange of a colour-singlet in the t -channel. In Regge theory¹ the colourless system exchanged at high energy is a universal trajectory with the quantum numbers of the vacuum, the Pomeron (IP), introduced to describe the energy dependence of the total cross sections in hadron-hadron scattering. In perturbative QCD (pQCD), the vacuum exchange is modelled as a two-gluon system that develops into a gluon ladder between the virtual photon and the proton. pQCD calculations are possible for diffractive processes where a hard scale is present: production of high mass quarks or high momentum jets, and, at HERA, ep scattering mediated by photons with high virtuality Q^2 .

In a diffractive DIS event, $e(k)p(P) \rightarrow e(k')XY(P')$, the photon dissociates into the hadronic state X, while the proton remains intact in the final state or dissociates in a low mass hadronic system Y that generally escapes undetected in the beam pipe. The two hadronic systems X and Y remain distinct in the final state.

In addition to the usual DIS variables, $Q^2 = -q^2 = -(k - k')^2$, $y = (P \cdot q)/(P \cdot k)$, $x = Q^2/(2P \cdot q)$, other quantities are used to describe the kinematics of a diffractive DIS event:

$$x_{IP} = \frac{q(P - P')}{qp} \simeq \frac{Q^2 + M_X^2}{Q^2 + W^2}, \quad t = (P - P')^2, \quad \beta = \frac{Q^2}{2q \cdot (P - P')} \simeq \frac{Q^2}{Q^2 + M_X^2}; \quad (1)$$

where M_X is the invariant mass of the dissociative photon system, $W^2 = (q + P)^2$ is the squared γ^*p centre of mass energy and $\beta = x/x_{IP}$. In resolved-Pomeron models, where a particle-like Pomeron is assumed to be emitted from the proton and the photon interacts with a partonic component of the Pomeron, x_{IP} is the fraction of the proton momentum carried by the Pomeron, and β is the fraction of the Pomeron momentum carried by the parton interacting with the virtual photon.

The QCD factorisation theorem proven for hard diffractive scattering² permits the definition of the differential cross section for the reaction $ep \rightarrow eXY$ in terms of a diffractive structure function F_2^D that depends on universal diffractive parton distributions:

$$\frac{d^4\sigma_{ep}^{diff}}{d\beta dQ^2 dx_{IP} dt} = \frac{2\pi\alpha^2}{\beta Q^4} (1 + (1-y)^2) F_2^{D(4)}(\beta, Q^2, x_{IP}, t). \quad (2)$$

If t is not measured, the above equation is integrated over t and the cross section is defined in terms of the diffractive structure function $F_2^{D(3)}(\beta, Q^2, x_{IP})$.

The measurements of the inclusive diffractive cross section in DIS^{3,4,5,6} are compatible with the resolved-Pomeron model of Ingelman and Schlein⁷ (IS) where the diffractive structure function factorises into a Pomeron flux factor, $f_{IP/p}(x_{IP}, t)$, and a Pomeron structure function, $F_2^{IP}(\beta, Q^2)$:

$$F_2^{D(4)}(\beta, Q^2, x_{IP}, t) = f_{IP/p}(x_{IP}, t) \cdot F_2^{IP}(\beta, Q^2). \quad (3)$$

The flux factor, describing the probability of finding a Pomeron in the proton as a function of x_{IP} and t , is parameterised according to Regge theory: $f_{IP/p}(x_{IP}, t) \sim x_{IP}^{1-2\alpha_{IP}(t)}$.

In the H1 analysis of inclusive diffractive data⁶ a QCD fit was performed in which the parton densities in the Pomeron were evolved according to the NLO DGLAP equations. The measured structure function $x_{IP} F_2^{D(3)}(\beta, Q^2, x_{IP})$, shown in Fig. 1(left) as a function of Q^2 for a fixed x_{IP} value and for different β bins, indicates a rising scaling violation, persisting also at relatively large values of β . This logarithmic scaling violation is described by the fit, which predicts a partonic momentum distribution in the Pomeron dominated by gluons.

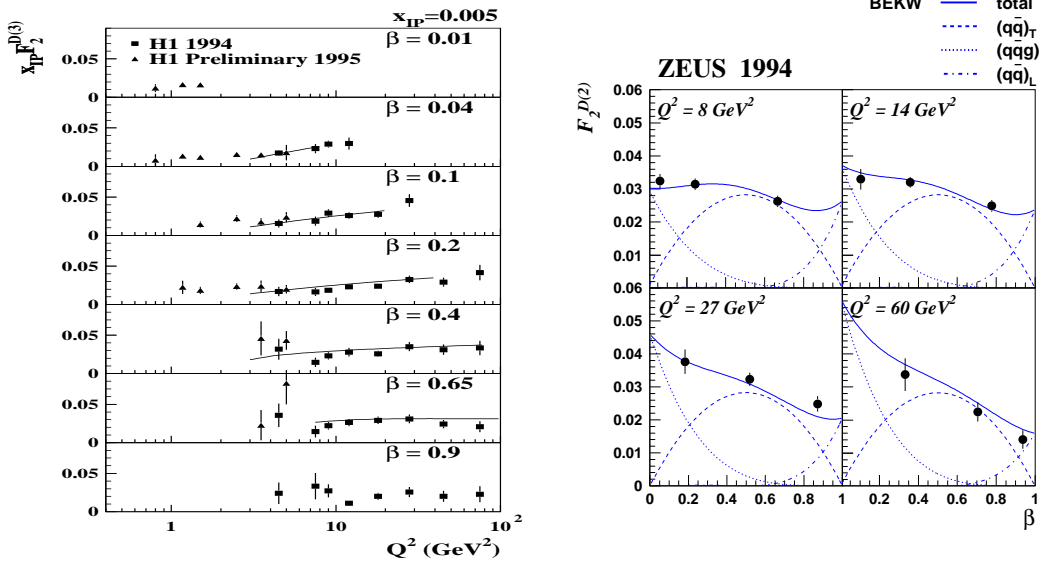


Figure 1: **Left:** H1 data on $x_{IP} F_2^{D(3)}(\beta, Q^2, x_{IP})|_{x_{IP}=0.005} = F_2^{D(2)}(\beta, Q^2)$ as a function of Q^2 for different β bins. The curve is the result of a DGLAP fit of the parton momentum distributions in the pomeron. **Right:** Comparison of the ZEUS data on $F_2^{D(2)}$ with a fit based on the BEKW model.

The approach in which the photon has a pointlike coupling with a partonic component of the Pomeron is valid in the proton infinite momentum frame. Diffractive γ^*p scattering can also be studied in the proton rest frame, where the virtual photon fluctuates into a hadronic state (a colour-dipole $q\bar{q}$ or higher Fock states) at large distances upstream of the proton target. The γ^*p cross section is factorised into the square of an effective dipole wave function (calculable in QED) and the cross section for the diffractive scattering of the dipole off the proton, which can be calculated in pQCD^{8,9,10,11} for high enough values of Q^2 .

The result of a fit based on a pQCD calculation of the dipole-proton cross section (BEKW model¹¹) to ZEUS data of inclusive diffraction¹² is shown in Fig. 1(right). In the BEKW model

the diffractive structure function is the sum of three leading contributions, corresponding to the $q\bar{q}$ production from transverse and longitudinal photons, and $q\bar{q}g$ production from transverse photons: $F_2^{D(3)}(\beta, Q^2, x_{IP}) = aF_{q\bar{q}}^T + bF_{q\bar{q}}^L + cF_{q\bar{q}g}^L$. The fit predicts that the dominant contributions at low β comes from the $q\bar{q}g$ fluctuations of the photon.

The dipole approach has been employed in the “*saturation model*” by Golec-Biernat and Wüsthoff¹³. In this model the dipole cross section is parameterised as a function of the transverse size of the dipole, with the cross section growing from the colour transparency regime at small radii (large Q^2) to a constant value at large radii. This model gives a good description of the inclusive proton structure function $F_2(x, Q^2)$, including the region of small Q^2 values, where a partonic model of the Pomeron or pQCD calculations cannot be applied.

The diffractive cross section has been recently measured in the transition region between photoproduction and DIS ($0.2 < Q^2 < 0.7 \text{ GeV}^2$)¹⁴, with the scattered positron detected in the small angle electron calorimeter (BPC) of ZEUS. The Q^2 dependence of $x_{IP}F_2^{D(3)}$ is shown in Fig. 2 for different W and M_X bins. A sharp change of the Q^2 dependence is observed: while at large Q^2 the data do not exhibit a strong Q^2 dependence, at low Q^2 the structure function $x_{IP}F_2^{D(3)}$ becomes approximately proportional to Q^2 . This behaviour, expected on the basis of the conservation of the electromagnetic current, is described by the saturation model when a contribution of $q\bar{q}g$ fluctuations of the photon is included. The curves shown in Fig. 2 are obtained using the same parameters of the model that successfully describe the inclusive F_2 data.

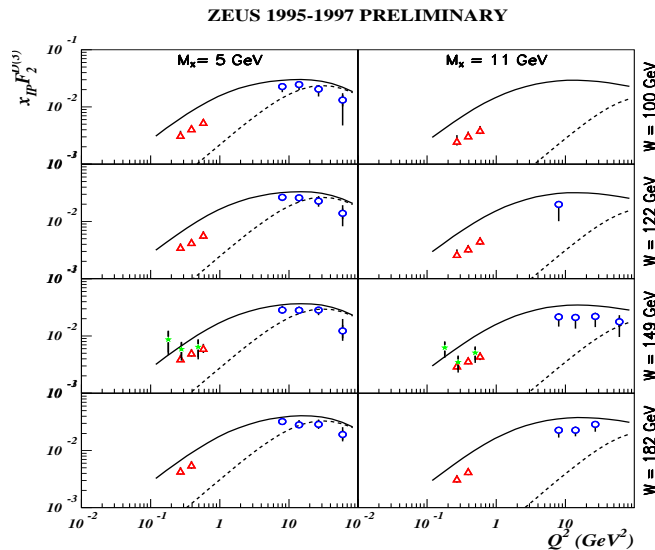


Figure 2: Values of $x_{IP}F_2^{D(3)}$ for different W and M_X bins as a function of Q^2 . The stars and the triangles indicate the measurements at low Q^2 with the BPC. The higher Q^2 points (open circles) are from previous ZEUS measurements. The curves show the prediction of the “*saturation model*” if only $q\bar{q}$ photon fluctuations are considered (*dashed curve*) and with both $q\bar{q}$ and $q\bar{q}g$ fluctuations included (*continuous curve*).

2 Diffractive jet production

To further improve the understanding of diffraction, studies of the diffractive final state are performed at HERA. In particular, final states containing high transverse momentum (p_T) jets are calculable in pQCD, and yield direct constraints on the shape of the gluon distribution of the Pomeron.

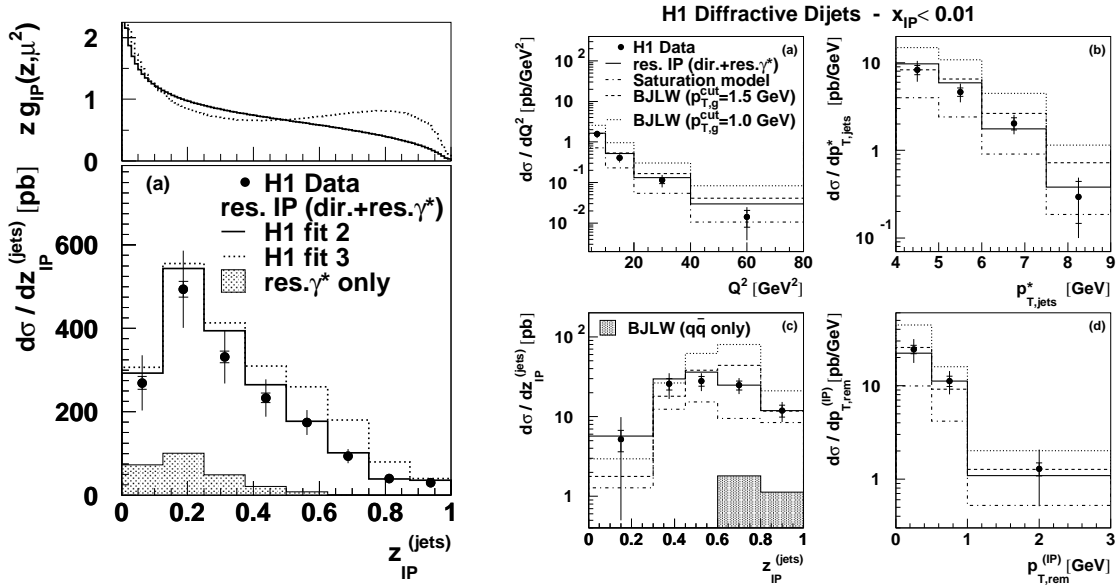


Figure 3: Di-jet production at H1. **Left:** diffractive dijet cross section as a function of z_{IP}^{jets} , compared with the prediction of the Ingelman-Schlein model for different gluon distributions. **Right:** differential diffractive dijet cross sections in the restricted kinematic range $x_{IP} < 0.01$ as a function of (a) Q^2 , (b) $p_{T,jets}^*$ (p_T of the jets calculated with respect to the γ^*p axis), (c) z_{IP}^{jets} (described in the text), (d) $p_{T,rem}^{(IP)}$ (the summed transverse momentum of the final state particles in the Pomeron hemisphere not belonging to the two jets).

In the H1 analysis¹⁵ DIS events with a large rapidity gap and at least 2 jets with $p_T > 4$ GeV were found using the cone-jet algorithm.

In Fig. 3(left) the quantity $z_{IP}^{jets} = (Q^2 + M_{12}^2)/(Q^2 + M_X^2)$, representing the fraction of the hadronic energy in the final state contained in the two jets, is compared with the prediction from the IS model based on different sets of Pomeron gluon distributions obtained from the leading order DGLAP analysis of $F_2^{D(3)}$ by H1. The data favour a Pomeron dominated by gluons with a gluon momentum distribution that is relatively flat in z_{IP}^{jets} .

Several differential distributions are compared in Fig. 3(right) with the IS model (res.IP in the figure), the saturation model and a pQCD calculation based on a dipole approach (BJLW model⁸). In the IS model the same flux factor and Pomeron structure functions describe both the inclusive diffractive data and the dijet distributions, consistent with the factorization hypothesis expressed by Eq. 3 and with the universality of the Pomeron parton distributions in ep scattering.

For diffractively scattered $q\bar{q}$ photon fluctuations, a distribution peaked at $z_{IP} \sim 1$ is expected in Fig. 3(left); the low values of z_{IP} measured in the two-jet sample imply the dominance of $q\bar{q}g$ over $q\bar{q}$ scattering in the proton rest frame picture. Furthermore, the high gluon content of the Pomeron favours a picture in which, in the proton infinite momentum frame, the dominant contribution is a Boson-Gluon Fusion process, with two jets and a gluon remnant in the final state. This picture is consistent with the F_2^D data shown in Fig. 1(right) where at low β (or high M_X) the contribution of $q\bar{q}g$ photon fluctuations is expected to dominate. In these events the gluon is emitted almost collinear to the γ^*IP axis in the Pomeron direction, with small p_T , while the two quarks are emitted in the photon emisphere.

In order to confirm the validity of this picture, three-jet production in diffractive DIS was studied by both H1¹⁵ and ZEUS¹⁶ collaborations. In the ZEUS analysis the exclusive k_T -algorithm¹⁷ was used in the centre of mass of the observed hadronic final state to select jet configurations aligned with respect to the γ^*IP axis. The measurement was restricted to high-mass final states ($M_X > 23$ GeV), in order to separate clear three-jets topologies, and diffractive

events were selected by requiring a large rapidity gap in the outgoing proton direction.

The energy flow, measured with respect to the azimuthal angle φ^* in the event plane defined by the two most energetic jets, is shown in Fig. 4(left). A clear three-jet structure, reproduced by different MC models, is observed.

The shapes of the jets were studied with the aim of distinguishing between quark and gluon-initiated jets. The differential jet shape $\rho(\varphi)$, defined as the average fraction of the energy of the jet which lies in an annulus of inner angular distance $\varphi - \delta\varphi/2$ and outer angular distance $\varphi + \delta\varphi/2$ around the jet axis, is shown in Fig. 4(right) as a function of φ for the most-forward and most-backward jet, where the forward direction is defined by the Pomeron direction. The measured jet in the Pomeron direction is broader than the jet in the photon direction, as expected for a jet initiated by a gluon preferentially emitted in the Pomeron direction. The jet shape distribution is reproduced by the RAPGAP MC model¹⁸, based on the resolved-Pomeron model with a Pomeron dominated by gluons.

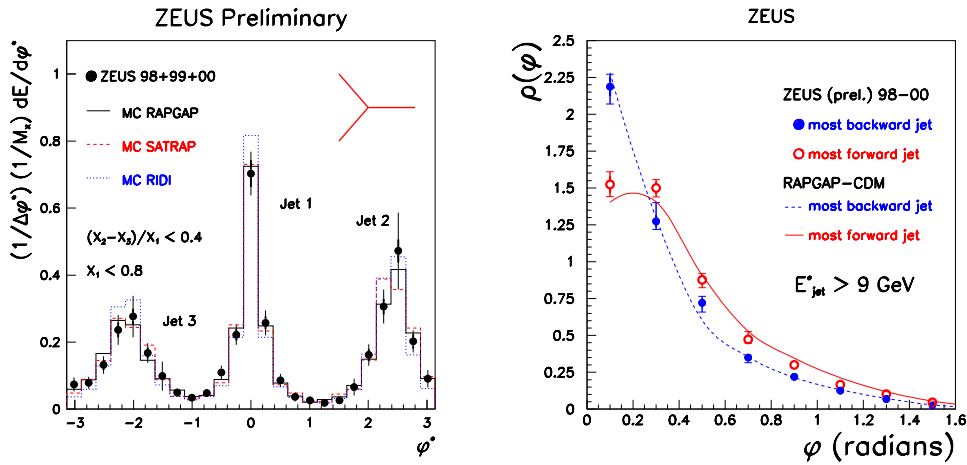


Figure 4: **Left:** Energy distribution normalized to the total invariant mass M_X as a function of the azimuthal angle φ^* defined in the plane of the two most energetic jets. **Right:** Differential jet shape for the most forward and most backward jet in three jets events with $E^{jet} > 9$ GeV.

3 Summary

Recent results on diffraction from HERA have been reviewed. The cross section has been presented in terms of the diffractive structure function F_2^D and the jet-structure of the hadronic final state X has been discussed. The data are described by models based on the Ingelman and Schlein approach, where the parton distributions in the Pomeron are probed, in the proton infinite momentum frame, by a pointlike virtual photon.

The data are also described in a consistent way by pQCD calculations in the proton rest frame, where the photon fluctuates into a colour dipole that interacts with the proton via the exchange of a gluon ladder; a dipole approach with the dipole-proton cross section parameterised as a function of the dipole radius describes the transition to low Q^2 .

In both points of view, three partons in the final state are expected at low β (or, equivalently, in events with high hadronic mass M_X), with a low- p_T gluon emitted preferentially in the Pomeron direction. Three jets events were observed at HERA, with a topology consistent with this picture.

1. P.D.B.Collins in “*An introduction to Regge theory and high energy physics*”, Cambridge Univ.Press, Cambridge (1977).
2. J.C.Collins, *Phys. Rev. D* **57**, 3051 (1998).
3. H1 Collab., T.Ahmed et al., *Phys. Lett. B* **348**, 681 (1995).
4. ZEUS Collab., M.Derrick et al., *Z. Phys. C* **68**, 569 (1995).
5. ZEUS Collab., J.Breitweg et al., *Eur.Phys.J. C* **1**, 81 (1998).
6. H1 Collab., C.Adloff et al., *Z. Phys. C* **76**, 613 (1997).
7. G.Ingelman and P.E.Schlein, *Phys. Lett. B* **152**, 256 (1985).
8. J.Bartels, H.Jung and M.Wüsthoff, *Eur.Phys.J* **11**, 111 (1999).
9. M.Genovese and N.N.Nikolaev, *J.Exp.Theor.Phys.* **81**, 633 (1995).
10. A.Bialas, R.Peschanski and C.Royon, *Phys. Rev. D* **57**, 6899 (1998).
11. J.Bartels, C.Ewerz, H.Lotter and M.Wüsthoff, *Phys. Lett. B* **386**, 389 (1996);
H.Lotter, *Phys. Lett. B* **406**, 171 (1997);
J.Bartels, J.Ellis, H.Kowalski and M.Wüsthoff, *Eur.Phys.J. C* **7**, 443 (1999).
12. ZEUS Coll., J.Breitweg et al., *Eur.Phys.J. C* **6**, 43 (1999).
13. K.Golec-Biernat and M.Wüsthoff, *Phys. Rev. D* **59**, 014017 (1999);
K.Golec-Biernat and M.Wüsthoff, *Phys. Rev. D* **60**, 114023 (1999).
14. ZEUS Coll., J.Breitweg et al., paper 435 submitted to the XXXth International Conference on High Energy Physics, Osaka, Japan (August 2000).
15. H1 Collab., C.Adloff et al., DESY 00-174, hep-ex/0012051.
16. ZEUS Coll., J.Breitweg et al., paper 433 submitted to the XXXth International Conference of High Energy Physics, Osaka, Japan (August 2000).
17. S.Catani et al., *Phys. Lett. B* **269**, 432 (1991)
18. H.Jung, *Comp.Phys.Comm.* **86** 147 (1995).